Vol 14 No 1, January 2005
1009-1963/2005/14(01)/0172-09

Chinese Physics

© 2005 Chin. Phys. Soc.
and IOP Publishing Ltd

D–T burning plasma characteristics in an A=2 tokamak reactor*

Shi Bing-Ren(石秉仁)†

Southwestern Institute of Physics, Chengdu 610041, *China*

(Received 14 May 2004; revised manuscript received 6 September 2004)

The deuterium–tritium (D–T) burning plasma characteristic in an aspect ratio A=2 tokamak reactor is studied based on a simple equilibrium configuration, the Soloviev-type configuration. Operation limits for the Troyon beta value and for the Greenwald density value as well as for the ITER H-mode confinement scaling are used as the benchmark. It is found that in addition to suitable elongation, large triangularity has advantage for arriving at high beta value and obtaining high fusion power output. Compared to the present ITER design, the A=2 system can have very good merit for the avoidance of disruptions by setting rather high edge q value while keeping relatively large total toroidal current. The main disadvantage of decreasing the aspect ratio is due to the loss of more useful space in the inward region that leads to the decrease of toroidal magnetic field in the plasma region, then worsening the fusion merit. Our analysis and calculation also present a trade-off in this respect. Due to simple equilibrium configuration assumed, some other important issues such as the bootstrap current alignment cannot be optimized. However, the present analysis can offer an insight into the advantages of the medium aspect ratio reactor system that is a blank in present-day tokamak study.

Keywords: A=2 tokamak, burning plasmas, Solov'ev configuration
PACC: 5255P, 5250, 5255G

1. Introduction

It can be said that achievements of the world-wide magnetic fusion research over the past 50 years have been condensed into a great fruit: the ITER design.[1] The acceptance of China and South Korea into its construction phase and the return of the US to ITER obviously indicate the common recognition that tokamak has the greatest opportunity for establishing the first commercial fusion power station. It is also commonly recognized that there are still many issues both in physics and in technology to be solved or improved. For symmetric toroidal confinement systems, the ITER–FEAT is an experimental reactor system with aspect ratio $A \approx 3$ and the spherical approach has aspect ratio near 1.4 (the ST system) and such a system allows for much higher stable beta value but the engineering aspects are rather formidable. Recently, some studies[2–5] have shown that for a tokamak system with aspect ratio A near 2, which is almost a blank in present experimental tokamak devices and in theoretical studies,[4] there are interesting merits, e.g., the much safer disruption-free operation, the higher fraction of bootstrap current, the competing cost even for a reactor system using normal magnets,[2] etc. Compared to the spherical tokamaks,[6] though some physical properties are less competitive, the engineering aspects are much more feasible. At any rate, it is interesting and meaningful to do somewhat deeper research in this respect.

In this paper, we use a simple tokamak equilibrium configuration, the well-known Solov'ev configuration,[7–9] which has been widely used in tokamak stability studies, to analyse the deuterium–tritium (D–T) burning characteristics of an A=2 tokamak reactor. The assumption of such sort of equilibrium configuration that corresponds to a quasi-uniform current profile will certainly restrict ourselves to clarifying the burning plasma quantities under special pressure profile and toroidal current profile, however, we still have room to identify some interesting merits of the D–T burning physics. In this way, analyses can be easily conducted. For burning condition analysis, we still use the general procedure used in

*Project supported by the National Natural Science Foundation of China (Grant No 10375018).
†E-mail: shibr@swip.ac.cn

tokamak reactor design. We set a certain limit for the Troyon beta factor $\beta_{\rm N}$ and the allowable Greenwald density factor $g_{\rm N}$ according to reasonable extrapolation of the present-day tokamak scaling. It will be shown that besides the suitable elongation effect which is thought to be beneficial for improving fusion reactor merit, the triangularity effect is very sensitive for improving burning characteristics. Several important features can be exploited in this relatively simple analysis.

2. Equilibrium property

2.1. Geometric relations

As usual, we assume the magnetic field in tokamak plasma to be

$$\boldsymbol{B} = \nabla\psi \times \nabla\zeta + F(\psi)\nabla\zeta, \tag{1}$$

where ψ is the poloidal magnetic flux function and $F = RB_{\rm t}$ the poloidal current function, ζ the toroidal angle. For quasi-uniform toroidal current distribution, i.e. by assuming $p'(\psi)$ and $F'^2(\psi)$ both to be constants, the Grad–Shafranov equation has a solution which corresponds to a special choice of a more general version:[7–9]

$$\psi = \frac{\psi_{\rm b}}{y_{\rm b}^2}\left\{\frac{4}{E^2}\left[1+(1-D)y\right]\frac{z^2}{R_0^2}+y^2\right\}, \tag{2}$$

where

$$y = \frac{R^2}{R_0^2} - 1, \tag{3}$$

R_0 is the major radius of the magnetic axis, parameter E is related to the elongation and D to the triangularity. If defining the inverse aspect ratio ε as the ratio of the half width of plasma cross section to the major radius of the geometric centre $R_{\rm p}$, we have the following relationships:

$$a_0 = \frac{R_0}{2}[\sqrt{1+y_{\rm b}} - \sqrt{1-y_{\rm b}}],$$

$$R_{\rm p} = \frac{R_0}{2}[\sqrt{1+y_{\rm b}} + \sqrt{1-y_{\rm b}}], \tag{4}$$

$$\varepsilon = \frac{\sqrt{1+y_{\rm b}} - \sqrt{1-y_{\rm b}}}{\sqrt{1+y_{\rm b}} + \sqrt{1-y_{\rm b}}}, \tag{5}$$

with

$$y_{\rm b} = \frac{2\varepsilon}{1+\varepsilon^2}. \tag{6}$$

We define the elongation and the triangularity as $\kappa = \dfrac{S_{\rm p}}{\pi a_0^2}$ ($S_{\rm p}$ is the area of cross-section) and $\delta = \dfrac{R_{\rm p} - R_*}{a_0}$ (R_* is the position where the cross section has its maximum z-value) respectively. These definitions give the following relationships:

$$\kappa = \frac{E y_{\rm b}^2 I_{\rm s}(y_{\rm b}, D)}{\pi(\sqrt{1+y_{\rm b}} - \sqrt{1-y_{\rm b}})^2}, \tag{7}$$

$$\delta = \frac{\sqrt{1+y_{\rm b}} + \sqrt{1-y_{\rm b}} - 2\sqrt{1+y_*}}{\sqrt{1+y_{\rm b}} - \sqrt{1-y_{\rm b}}}. \tag{8}$$

In Eq.(7),

$$I_{\rm s} = \int_{-\pi/2}^{\pi/2} \frac{{\rm d}t}{\sqrt{(1+y_{\rm b})\sin t(1+(1-D)y_{\rm b}\sin t)}}. \tag{9}$$

In Eq.(8),

$$y_* = \sqrt{\left(\frac{1}{1-D}\right)^2 - y_{\rm b}^2} - \frac{1}{1-D}. \tag{10}$$

We indicate that while the elongation only slowly varies with D, the triangularity rather sensitively depends on the parameter D. For a fixed aspect ratio, a negative D value makes the cross section rapidly change inboard. A typical example of equilibrium configurations for different choice of D is shown in Fig.1. Dependence of elongation and triangularity on D is shown in Fig.2.

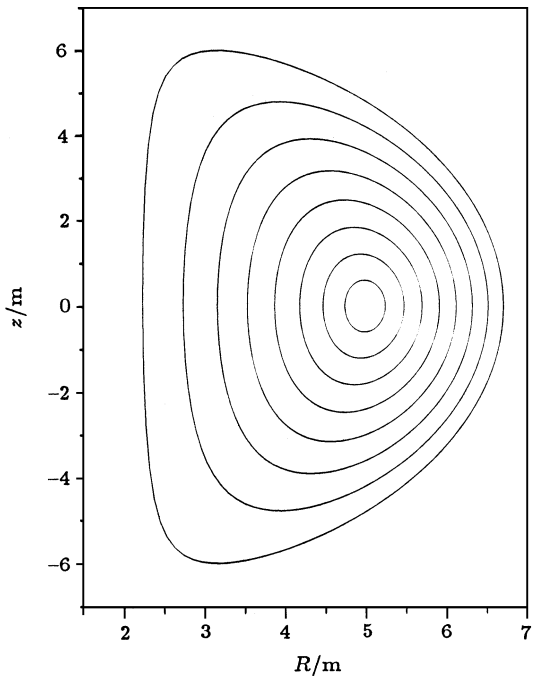


Fig.1. Magnetic surface contours for E=2.0, D=–0.2, ε=0.5 and R_0=5m.

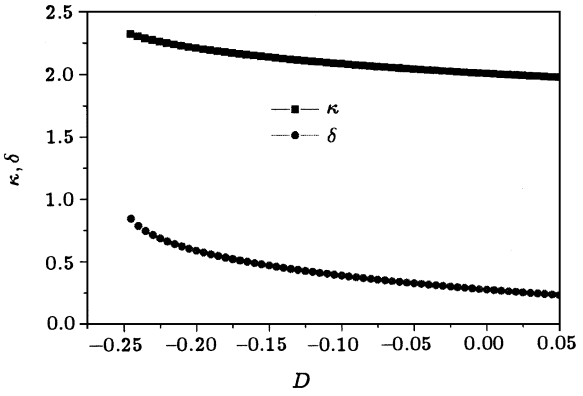


Fig.2. Curves of κ (upper), δ (lower) versus D for ε=0.5, E=2.0.

2.2. Safety factor profile

For the above-mentioned equilibrium, the safety factor q can be expressed as

$$q(\psi) = \left(\frac{F}{2\pi}\right)\left(\frac{Ey_{\rm b}^2 R_0}{4\psi_{\rm b}}\right) I_1(y_{\rm b}, D), \qquad (11)$$

where

$$I_1(y_{\rm b}, D) = \int_{-1}^{1} \frac{{\rm d}u}{(1+y_\psi u)\sqrt{[1+(1-D)y_\psi u](1-u^2)}}, \qquad (12)$$

and

$$y_\psi = y_{\rm b}\sqrt{\frac{\psi}{\psi_{\rm b}}}. \qquad (13)$$

The total toroidal current can be expressed as

$$I_{\rm p} = \frac{4E\psi_{\rm b}}{\mu_0 R_0}\left[\left(1+\frac{1-D}{E^2}\right)I_2 + \frac{D}{E^2}I_3\right], \qquad (14)$$

where the two integrals I_2 and I_3 are defined as follows:

$$I_2(y_{\rm b}, D) = \int_{-1}^{1} {\rm d}u\sqrt{\frac{1-u^2}{1+(1-D)y_{\rm b}u}}, \qquad (15)$$

$$I_3(y_{\rm b}, D) = \int_{-1}^{1} \frac{{\rm d}u}{1+y_{\rm b}u}\sqrt{\frac{1-u^2}{1+(1-D)y_{\rm b}u}}. \qquad (16)$$

Then the edge q value $q_{\rm ed}$ can be related to the total toroidal current $I_{\rm p}$ by

$$\frac{q_{\rm ed}I_{\rm p}}{F} = \frac{E^2 y_{\rm b}^2}{2\pi\mu_0} I_1\left[\left(1+\frac{1-D}{E^2}\right)I_2 + \frac{D}{E^2}I_3\right]. \qquad (17)$$

In the large aspect ratio case, the q-profile is rather flat. In the small aspect ratio case, however, the edge q value can be much higher than the central value. Besides, the shear value can be very large in the edge region as well.[7] This merit usually shows a good stability margin for ballooning modes. For different D, q-profiles are shown in Fig.3. To this end, we can recall an expression for the same quantity appearing in the left-hand side of Eq.(17) from a well-known fitting formula,[1,6] i.e.

$$\frac{q_{95}I_{\rm p}}{F} = 2.5\varepsilon^2[1+\kappa^2(1+2\delta^2-1.22\delta^3)]f(\varepsilon), \qquad (18)$$

where

$$f(\varepsilon) = \frac{1.17-0.65\varepsilon}{(1-\varepsilon^2)^2}. \qquad (19)$$

When we compare this quantity from the exact formula (17) with that from the fitting formulae (18) and (19), we find that the dependence of this quantity upon the inverse aspect ratio is consistent while the dependence upon the elongation and the triangularity diverges if these parameters are relatively large. Usually, the former is greater than the latter (see Fig.4).

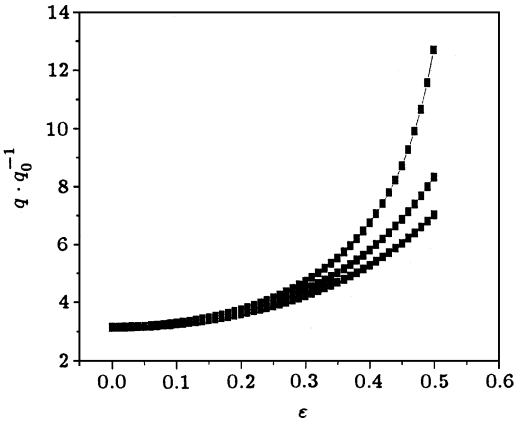


Fig.3. The q-profiles for different D, from the upper to the lower: D=–0.2, 0, 0.2.

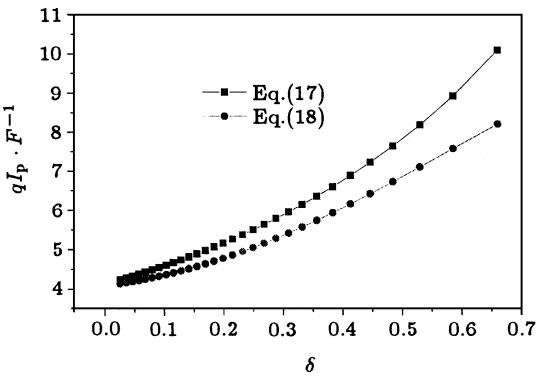


Fig.4. Comparison of the two values of $(q_{\rm ed}I_{\rm p}/F)$ from the accurate formula (17) and the fitting formula (18) for ε=0.5, E= 2.0.

2.3. Pressure profile

The Solov'ev configuration expressed in Eq.(2) determines the pressure profile (that is a relatively flat one compared to some other equilibrium cases) and the F function as follows:

$$P(\psi) = P_0\left(1 - \frac{\psi}{\psi_\mathrm{b}}\right), \tag{20}$$

$$F(\psi) = \left\{F_\mathrm{b}^2 + F_1^2\left(1 - \frac{\psi}{\psi_\mathrm{b}}\right)\right\}^{1/2}, \tag{21}$$

with

$$P_0 = \frac{8\psi_\mathrm{b}^2}{\mu_0 y_\mathrm{b}^2 R_0^4}\left(1 + \frac{1-D}{E^2}\right), \tag{22}$$

$$F_1^2 = \frac{16D\psi_\mathrm{b}^2}{y_\mathrm{b}^2 E^2 R_0^2}. \tag{23}$$

We assume that both the density and temperatures of the electron and the ion are flux functions and neglect the contribution of the fusion alpha particle pressure at the moment (noting that this part of pressure profile cannot fit the form expressed in Eq.(20)). Then we write the density and the temperature profile as

$$n_\mathrm{e} = n_{\mathrm{e}0}\left(1 - \frac{\psi}{\psi_\mathrm{b}}\right)^{\alpha}, \tag{24}$$

$$T_\mathrm{e} = \tau_\mathrm{e} T_\mathrm{i} = T_{\mathrm{e}0}\left(1 - \frac{\psi}{\psi_\mathrm{b}}\right)^{1-\alpha}, \tag{25}$$

and the temperature ratio τ_e is taken to be constant for simplicity.

2.4. Relationship with operation limit

As is well known, the tokamak suffers from some operation limits, such as the density limit and the beta limit. For the former, the so-called Greenwald limit[10] refers to

$$< n_\mathrm{e} >= k_\mathrm{G}\frac{I_\mathrm{p}}{\pi a_0^2}. \tag{26}$$

For the beta limit, the Troyon factor[11] is described as

$$\beta_\mathrm{N} = 100\beta\frac{a_0 B_\mathrm{t}}{I_\mathrm{p}}. \tag{27}$$

In what follows, we select q_ed as a basic parameter that restricts the total toroidal current, then we obtain the central beta value as

$$\beta_0 = \left(\frac{E y_\mathrm{b} I_1}{2\pi q_\mathrm{ed}}\right)^2\left(1 + \frac{1-D}{E^2}\right). \tag{28}$$

By combining Eqs.(14) and (25) and using the definition of a_0, the Troyon factor can be written as

$$\beta_\mathrm{N} = \frac{20 c_\beta \varepsilon I_1}{q_\mathrm{ed}[I_2 + DI_3/(E^2+1-D)]}, \tag{29}$$

where $c_\beta =< \beta > /\beta_0$. Now we see that β_N is proportional to $(\varepsilon/q_\mathrm{ed})$ and depends sensitively on parameter D through I_1 which, for a configuration with relatively large δ and β_N, can be very high. For a given β_N, the Greenwald limit gives the central electron density as

$$n_{\mathrm{e}0} = \frac{k_\mathrm{G}\beta_\mathrm{N} B_\mathrm{t} E^2 y_\mathrm{b}^2}{16\pi^3 c_\mathrm{n} c_\beta \varepsilon^2 a_0}\left(1 + \frac{1-D}{E^2}\right) \times \left[I_2 + \frac{D}{E^2+1-D}I_3\right]^2. \tag{30}$$

In turn, using $\beta_0 = 2\mu_0 n_{\mathrm{e}0}(T_{\mathrm{e}0} + T_{\mathrm{i}0})/B_\mathrm{t}^2$, the central ion temperature is then obtained according to Eqs.(28)–(30). It is noted that all the above quantities are functions of the equilibrium parameters E, D and ε (or y_b). In particular, they depend on the triangularity parameter D very sensitively.

2.5. Some remarks on the equilibrium

The Solov'ev equilibrium is peculiar in some respects. We can find that the Shafranov shift does not depend on the pressure gradient. This is because in this equilibrium, a change in the pressure gradient would simultaneously cause a change of the toroidal current, and then the poloidal beta value keeps constant. In turn, the central toroidal beta exhibits a relationship with the total current appearing in Eq.(28). (In general, the pressure gradient and the toroidal current can be selected as independent input parameters.) This peculiarity makes it impossible to compare the results with other burning characteristics carried out below, e.g. the ITER-FEAT parameters. However, we still can compare the results obtained from cases of different aspect ratios if they have the same equilibrium configuration.

3. D–T burning characteristic

The thermal energy density of the D–T burning plasma is

$$w_\mathrm{p} = \frac{3}{2}n_\mathrm{e}(T_\mathrm{e} + T_\mathrm{i}). \tag{31}$$

The fusion-produced alpha particle power density is

$$p_\alpha = \frac{1}{4}n_\mathrm{e}^2 f_\mathrm{DT}^2 < \sigma v >_\mathrm{DT} E_\alpha, \tag{32}$$

where f_DT is the D–T ion dilution factor due to impurity contents. We use the Hively formula[12] as the D–T fusion reaction rate function:

$$< \sigma v >_\mathrm{DT} = \exp\left\{\frac{a_1}{T^\gamma} + a_2 + a_3 T + a_4 T^2 + a_5 T^3 + a_6 T^4\right\}, \tag{33}$$

with $\gamma = 0.2935$, $a_1 = -21.377692$, $a_2 = -25.204254$, a_3=–0.071013427, a_4=1.9374541×10^{-4}, a_5=4.9246592×10^{-6}, a_6=–3.9836572×10^{-8}.

The unit of the ion temperature in this formula is keV, and that of the reaction rate is $cm^3 \cdot s^{-1}$.

For the radiation loss, we only consider the bremsstrahlung, and use the following formula:

$$p_{\rm brem} = 1.68 \times 10^{-2} n_{\rm e0}^2 Z_{\rm eff} T_{\rm e0}^{1/2}, \qquad (34)$$

where $T_{\rm e}$ is in unit of 10keV while p in $MW \cdot m^{-3}$.

We use zero-dimensional energy balance analysis so that the above quantities in Eqs.(30)–(33) should be integrated over the total plasma volume. This integration can be carried out according to the following regulation:

$$\iiint {\rm d}\tau U(\psi, R) = \frac{\pi y_{\rm b}^2 E R_0^3}{2} \int_0^1 {\rm d}t \int_{-1}^1 {\rm d}u \times \frac{U(\psi_{\rm b} t, R)}{\sqrt{(1-u^2)(1+(1-D)y_{\rm b} t u)}}. \qquad (35)$$

In particular, for U =1, we obtain the plasma volume. Usually, these volume integrations are proportional to ER_0^3 while not sensitively depending on the choice of D.

For the confinement scaling, the IPB98(y, 2) ELMy H-mode scaling in the ITER design[1] is also used here:

$$\tau_E = 0.144 H_{\rm h} P_{\rm t}^{-0.69} B_{\rm t}^{0.15} I_{\rm p}^{0.93} \kappa^{0.78} < n >^{0.41} a^{0.58} R^{1.39} M^{0.19}. \qquad (36)$$

In what follows, we are faced with a multi-parameter optimization. Anyway, we should fix some parameters first according to physical considerations. In the present investigation, we set the aspect ratio $A = 2$ or $y_{\rm b}$=0.8. For the elongation which is very beneficial for improving the confinement and for better reactor merit, we use a scaling as in Refs.[2,3]:

$$\kappa = 1.082 + 2.747/A. \qquad (37)$$

This gives $\kappa = 2.46$ for $A = 2$. In the following we set E=2.0 ($\kappa \approx 2.2$). In the case with this aspect ratio, the largest choice of triangularity is given by setting $D = -0.25$ and $\delta \to 1.0$. Conservatively, we set $D = -0.2$ and $\delta \approx 0.58$ in the following analysis but results to be compared will also be given for another choice of D.

3.1. Case I: ITER–FEAT-like size

We first consider a case that the major radius of the reactor equals that of the ITER–FEAT, i.e. $R_{\rm p}$=6.2m, corresponding to R_0=6.93m and $a_{\rm p}$=3.1m. Of course, this choice makes the plasma volume in this reactor larger than that of the ITER–FEAT. For the Troyon beta factor, in Refs.[2,3] the DIII-D high equivalent DT yield result[13,14] refers to

$$\beta_{\rm N} = \frac{(3.09 + 3.35/A + 3.87/\sqrt{A})}{\text{peak factor}^{0.5}} \left(\frac{\kappa}{3}\right)^{0.5}. \qquad (38)$$

It is noted that the equilibrium configuration discussed here is quite different from the DIII-D case; however, the D–T burning characteristic does not sensitively depend on the equilibrium profile for zero-dimensional analysis. The above formula gives an uppermost value of the allowable $\beta_{\rm N}$=4.6; here we set $\beta_{\rm N}$=4.0 (we note that in the recent NSTX experiments[14] with A=1.4, κ=2.0, δ=0.8, high beta plasmas with $\beta_{\rm N} = 6$ were already routinely achieved while Eq.(38) predicts $\beta_{\rm N} \approx 5.0$ for a peak-factor =2).

3.2. Commercial reactor case

This case basically corresponds to a D–T power station with output of 1GW(e) (with the fusion power around 3GW) so that the size should be rather large.

Obviously, the reactor design study needs a system code such as that used in the ITER design.[15] Here we can only use some fundamental scientific consideration to estimate relevant issues instead. One important issue is the allowable toroidal magnetic strength that is basically determined by the available super-conducting magnet technology on the one hand and the toroidal geometry of the reactor on the other. If the maximum allowable magnetic strength of the super-conducting magnet is $B_{\rm m}$, the magnetic field at the reactor centre will be

$$B_{\rm t} = B_{\rm m}\left(1 - \frac{a_{\rm p} + L_{\rm x}}{R_{\rm p}}\right), \qquad (39)$$

with $L_{\rm x}$ being the thickness of the blanket plus the shielding material layer. In the following we take $L_{\rm x}$=1.2–1.4m depending on how large the reactor scale is. For the case 3.1, i.e. the ITER–FEAT size case, we assume $B_{\rm m}$=11T, and $L_{\rm x}$=1.2m. For $R_{\rm p}$=6.2m, we have $B_{\rm t}$=3.37T.

4. Typical results

4.1. For the case 3.1

The reduction of the aspect ratio from 3.1 to nearly 2 makes the edge q value much larger for similar or even larger total toroidal current compared to the ITER–FEAT value q_{ed}=3 and I_p=15MA, this means a much safer disruption-less operation. Other relevant quantities are listed in Table 1 for H_h=1.0.

Because the decrease in aspect ratio makes the inboard space much tighter, the deceased magnetic field is predicted if equivalent technology of the magnet system is foreseen. We choose lower B_t than that in the present ITER–FEAT. Three cases are shown in Table 1. Self-sustaining burning cannot be realized in this case. The last row in this table shows that to arrive at a self-sustaining burning, how large the value of H_h^*, the enhancement factor over the ITER H-mode scaling should be. We find that the increase in magnetic field is beneficial for improving fusion merit. (The fusion alpha power and the fusion performance $Q_{fus} = 5P_\alpha/P_h$ versus B_t are shown in Fig.5.) Generally, reactors in this parameter range does not show much better benefits than the present ITER–FEAT case (A=6.2/2) except for the much larger edge q that makes disruption-free operation much more practical.

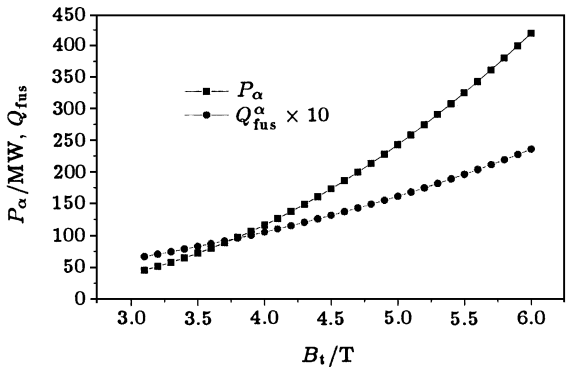


Fig.5. The alpha power and Q_{fus} versus B_t for the ITER–FEAT size case.

4.2. In the commercial reactor case of 3.2

We mainly consider the self-sustaining burning condition if the H-mode enhancement factor can be larger than 1. We keep ε=0.5, κ=2.2, δ=0.5 as in the case of 3.1, the major radius increases to about or larger than R_p=9.0m. Other parameters are shown in Table 2.

It can be seen that in this case, the reactor should operate at a rather high ion temperature while the density is still relatively low. This is basically due to the Greenwald density limit that strongly restricts the corresponding averaged density. In this case, rather high ion temperature is required. This is certainly not beneficial for obtaining high fusion gain; on the other hand, the high temperature operation would lead to formidable edge conditions. To alleviate this disadvantage, it is anticipated to operate at high Greenwald value. The possibility to do so has been verified in experiments.[16] In Figs.6 and 7 are shown the dependences of the fusion alpha power, the central density and the ion temperature on the Greenwald index k_G, respectively.

Table 1. The parameters in the ITER–FEAT size reactor case.

$R_p \cdot \alpha_p^{-1}$/m	6.2 / 3.1	κ/δ	2.2 / 0.58
q_{ed}/q_0	8.8 / 2	β_N/τ_e	4.0 / 1.1
α_n/α_T	0.5/0.5	f_{DT}/Z_{eff}	0.85 / 1.7
B_t/T	3.37	I_p/MA	21.5
k_G	0.85	1.0	1.15
$n_{e0}/10^{20}$m^{-3}	0.95	1.12	1.29
T_{i0}/10keV	2.48	2.11	1.84
P_α/MW	101	107	109
P_h/MW	55.1	48.3	43.5
Q_{fus}	9.2	11.1	12.5
τ_E/s	9.23	9.49	9.94
H_h^*	1.61	1.52	1.48

Table 2. Commercial reactor case.

κ/δ	2.2 / 0.58	ε	0.5
q_{ed}/q_0	10.0 / 2.48	β_N/τ_e	4.0 / 1.1
α_n/α_T	0.5 / 0.5	f_{DT}/Z_{eff}	0.85 / 1.7
R_p/a	8.9 /4.5	9.8 /4.9	10.8 /5.4
B_t/T	3.9	4.05	4.1
I_p/MA	36.0	41.1	45.4
k_G	1.15	1.0	0.85
$n_{e0}/10^{20}$m^{-3}	1.03	0.84	0.67
T_{i0}/10keV	3.08	4.04	5.34
P_α/MW	483	569	571
P_h/MW	51.9	98.8	180
Q_{fus}	46.6	28.8	15.8
τ_E/s	11.1	12.6	15.2
H_h^*	1.12	1.19	1.34

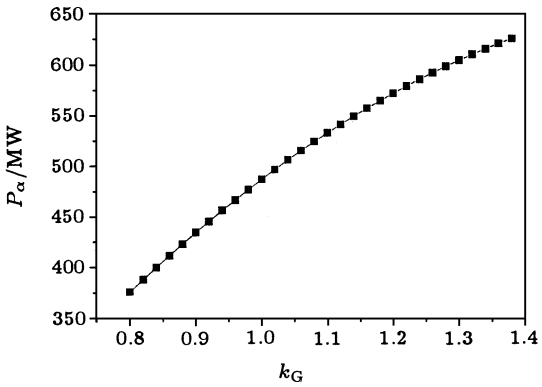


Fig.6. The fusion alpha power versus k_G for the case of 3.2; other parameters corresponds to the second column of Table 2.

There will be other questions for high ion temperature operation in tokamak systems; e.g., the raised electron synchrotron radiation might increase the radiation loss that we did not take into account in the above calculation. We hope to seek relatively lower temperature regime through the increase in the plasma density. This will be discussed in the next section.

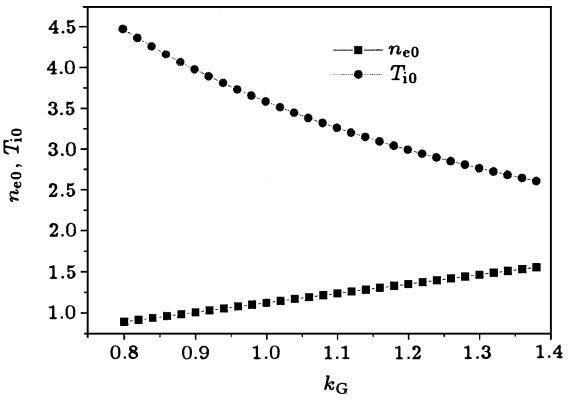


Fig.7. For the case of 3.2, the central density and the ion temperature versus k_G. Other parameters are the same as in Fig.6.

5. Advanced shaping operation

To increase the density, it is necessary to increase the toroidal current. The direct way is to raise the elongation. This needs an advanced shaping technique to stabilize the vertical instability. From the scaling formula (37) it is anticipated that for an A=2 reactor, the elongation can be as high as κ=2.46. In the above calculation we only take κ=2.2. In the following, we assume that the advanced stabilizing technique can realize $\kappa \leq 2.7$. The benefit is remarkable. We still discuss the self-sustaining burning case for $H_h < 1$. The β_N value is still kept at 4.0. The magnetic field is determined by Eq.(39) where B_m =11T and L_x=1.3m are fixed as the basic technical requirement. The total toroidal current (and the edge q value) are almost the same for the three examples. A combination of somewhat higher Greenwald coefficient ($k_G > 1.0$) and higher elongation ($\kappa > 2.3$) can make the self-sustaining burning feasible. Typical examples are listed in Table 3. We find that for $\kappa > 2.4$ self-sustaining burning is reached and the general feature for the requirement of enhancement factor versus E is shown in Fig.8. The total fusion alpha power versus the elongation parameter E is also remarkable. (Fig.9).

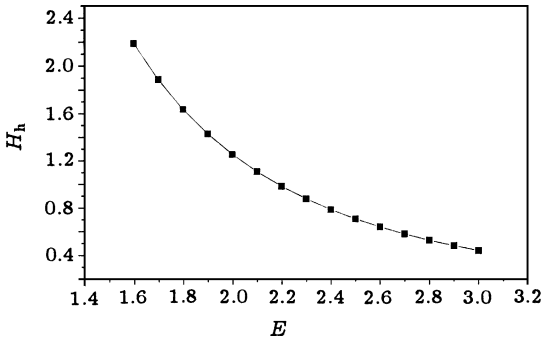


Fig.8. Self-sustaining condition for the enhancement factor H_h versus E for an advanced shaping case. Other parameters can be found in Table 3 (ii).

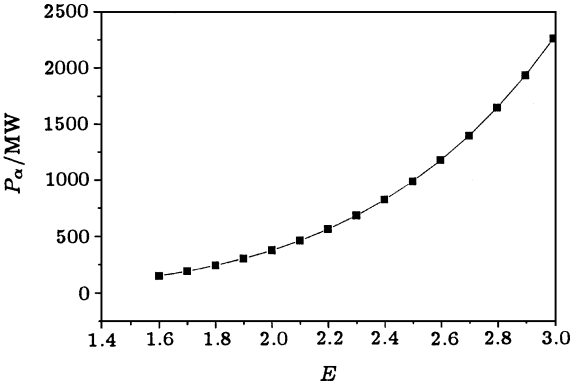


Fig.9. The output fusion alpha power versus E (the advanced shaping case).

In Table 3 are shown three combinations of the major radius and the elongation: (i) E =2.4 (κ=2.65), R_p=8.05m; (ii) E =2.3 (κ=2.57) R_p=8.5m; (iii) E=2.2 (κ=2.43), R_p=8.94m and other fixed or almost fixed parameters are: $D = -0.2(\delta = 0.5)$, A=2, β_N= 4.0, α=0.5, k_G=1.0, τ_e = 1.1, $q_{ed} \approx 6.7$, $I_p \approx$0.43MA.

Table 3. Self-sustaining burning case of a commercial reactor.

	(i)	(ii)	(iii)
R_p/m	8.05	8.5	8.94
κ	2.65	2.57	2.43
q_{ed}	8.64	8.67	8.7
$n_{e0}/10^{20}$m^{-3}	1.31	1.18	1.06
T_{i0}/10keV	3.04	3.29	3.54
I_p/MA	42.7	42.8	42.5
V_p/m^3	2658	3126	3646
W_p/GJ	6.2	6.6	7.1
P_α/MJ	675	675	655
τ_E/s	12.3	12.3	12.4
H_h	0.80	0.87	0.96

Finally, we consider how the variation of β_N would change the fusion characteristic. We choose a little higher magnetic field B_t=4.5T for this case. Results

are shown in Figs.10–12 for the toroidal current, the alpha power, and the central density and the ion temperature as functions of β_N respectively. Other parameters are R_p=8.05m, B_t=4.5T, E =2.2. It can be seen that 3GW fusion power can be obtained for $\beta_N \geq 3.5$: that is, the basic choice of our calculations above.

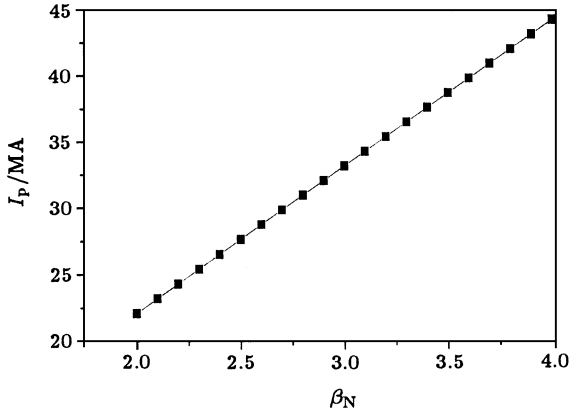


Fig.10. I_p versus β_N for a reactor with parameters: R_p=8.05m, B_t=4.5T, E=2.2.

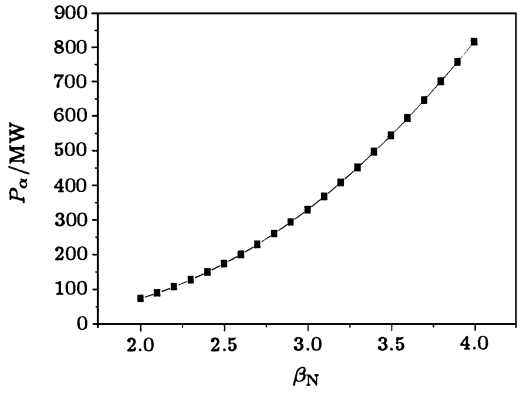


Fig.11. The alpha power versus β_N, parameters are the same as in Fig.10.

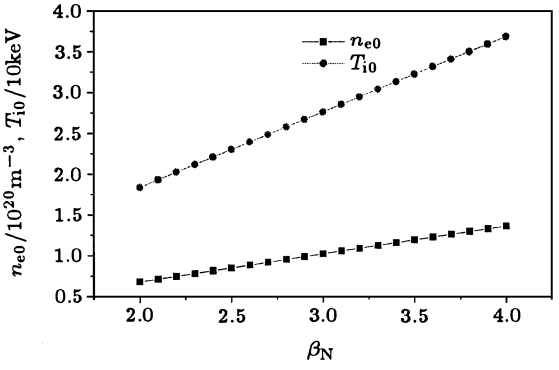


Fig.12. n_{e0} and T_{i0} versus β_N, parameters are the same as in Fig.10.

6. Bootstrap current fraction

It is well known that the bootstrap current profile has a hollow form so that our assumption of quasi-uniformity is not well aligned with it. However, the total bootstrap current does not sensitively depend upon the equilibrium detail so we can calculate the bootstrap fraction by our simple equilibrium model, which has the merit of being able to change the aspect ratio, the elongation and the triangularity easily. Now we write the toroidal current density as[16]

$$j_\zeta = -R\frac{\mathrm{d}p}{\mathrm{d}\psi}\left[1-\frac{F^2}{R^2<B^2>}\right] + \frac{<jB>F}{R<B^2>}. \tag{40}$$

Then the fraction of the bootstrap toroidal current density is given by

$$j_{bs} = \frac{<jB>_{bs}F}{R<B^2>}. \tag{41}$$

The symbol <> denotes the surface average; in our terminology, it reads

$$<U>=\frac{\int_0^\pi \frac{U\mathrm{d}u}{\sqrt{1+(1-D)y_\psi\cos u}}}{\int_0^\pi \frac{\mathrm{d}u}{\sqrt{1+(1-D)y_\psi\cos u}}}. \tag{42}$$

In the following, as is usually the case, we assume that $F \gg |\nabla\psi|$, then we have $<B^2>\approx F^2<1/R^2>$, and the total bootstrap current becomes

$$\begin{aligned} I_{bs} &= \int_0^{\psi_b}\mathrm{d}\psi\frac{<jB>_{bs}}{F}<\frac{1}{R^2}>\oint\frac{\mathrm{d}l_p}{B_p} \\ &= \frac{ER_0y_b^2}{2}\int_0^1\mathrm{d}x\frac{<jB>_{bs}}{F}\int_0^\pi \\ &\quad\times\frac{\mathrm{d}u}{\sqrt{1+(1-D)y_b\sqrt{x}\cos u}}. \end{aligned} \tag{43}$$

For the expression of the parallel component of the bootstrap current, here we select the single ion, collisionless model [16,17] as

$$<jB>_{bs} = -Fp_e\left\{\frac{A_1}{p_e}\left[\frac{\mathrm{d}p_e}{\mathrm{d}\psi}+\frac{\mathrm{d}p_i}{\mathrm{d}\psi}-\alpha_i n_i\frac{\mathrm{d}T_i}{\mathrm{d}\psi}\right] - \frac{A_2}{T_e}\frac{\mathrm{d}T_e}{\mathrm{d}\psi}\right\}, \tag{44}$$

with

$$\begin{aligned} A_1 &= [x(0.754+2.21Z+Z^2) \\ &\quad + x^2(0.347+1.24Z+Z^2)]/D_e, \\ A_2 &= x(0.885+2.08Z)/D_e, \\ D_e &= 1.41Z+Z^2+x(0.775+2.65Z+2.0Z^2) \\ &\quad + x^2(0.347+1.24Z+Z^2), \\ \alpha_i &= 1.17/(1.0+0.46x). \end{aligned} \tag{45}$$

and

$$x = (1.46\sqrt{\varepsilon} + 2.4\varepsilon)/(1-\varepsilon)^{3/2}. \quad (46)$$

Now all quantities appearing in the above can be obtained for any set of equilibrium parameters and burning plasma parameters. After conducting some relatively simple integrations, we can obtain the bootstrap current fraction as a function of ε, E, D, R_0, by using Eqs.(20)–(25) and (15); the bootstrap fraction $f_{\rm bs}$ can be expressed in terms of relevant integrals as

$$\begin{aligned} f_{\rm bs} =& \frac{I_{\rm bs}}{I_{\rm p}} \\ =& \left\{ {\rm BS1} + \frac{1-\alpha_{\rm n}}{1+\tau_{\rm i}} {\rm BS2} \right. \\ & \left. - \frac{(1-\alpha_{\rm n})\tau_{\rm i}}{1+\tau_{\rm i}} {\rm BS3} \right\} / [2I_2 + 2DI_3/(1+E^2-D)], \end{aligned} \quad (47)$$

where

$$\begin{aligned} {\rm BS1} &= \int_0^1 {\rm d}t A_1 I_0, \\ {\rm BS2} &= \int_0^1 {\rm d}t A_2 I_0, \\ {\rm BS3} &= \int_0^1 {\rm d}t \alpha_{\rm i} A_1 I_0, \end{aligned} \quad (48)$$

and

$$I_0 = \int_0^{\pi} \frac{{\rm d}u}{\sqrt{1+(1-D)y_{\rm b}\sqrt{t}\cos u}}. \quad (49)$$

Now we find that though the total bootstrap current is proportional to the pressure of the D–T burning plasma, i.e. $I_{\rm bs} \propto P_0$, the fraction is only a function of the geometric parameters. It seems that the large triangularity has some benefit for the increase of the bootstrap fraction. In Fig.13 is shown the dependence of $f_{\rm bs}$ on D.

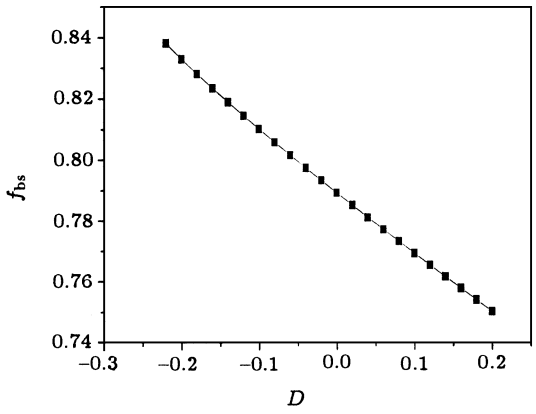


Fig.13. Dependence of the bootstrap current fraction on D for an A=2 Solov'ev configuration.

7. Discussion

In both the ITER–FEAT size case and the commercial reactor case with an aspect ratio A=2, one of the unique points is the edge q being much larger than the conventional tokamak with $A \geq 3$. This makes the burning plasma much more stable against the disruptions. However, this is obtained at the cost of lowering the magnetic field in the plasma centre. The second important point is the higher obtainable $\beta_{\rm N}$, due to the Greenwald density limit; however, this leads to higher temperature operation that is not hopeful in the present technology. If higher Greenwald value can be realized, or if advanced shaping is available, the A=2 tokamak reactor might be very competitive. It is worth studying in the future. Finally, some recent studies[18,19] should be noted that are to some extent related to this paper.

References

[1] The ITER Physics Basic Editors 1999 *Nucl. Fusion* **39** 2251

[2] Wong C P C, Wesley J C, Stambaugh R D *et al* 2002 *Nucl. Fusion* **42** 547

[3] Wong C P C and Stambaugh R D 2000 *Fusion Eng. Design* **51-52** 387

[4] Li Z W 2002 *Chin. Nucl. Fusion Plasma Phys.* **22** 86

[5] Shi B R 2003 *Chin. J. Nucl. Fusion Plasma Phys.* **23** 129 (in Chinese)

[6] Peng Y K M *et al* 1998 *25th EPS Conf. Control. Fusion Plasma Phys.* 1038

[7] Solov'ev L S 1968 *Sov. Phys. JETP* **26** 400

[8] Shi B R 2003 *Plasma Sci. Technol.* **5** 1849

[9] Weening R H 2000 *Phys. Plasmas* **7** 3654
Weening R H 1997 *Phys. Plasmas* **4** 3254

[10] Greenwald M 1988 *Nucl. Fusion* **28** 2199

[11] Troyon F 1983 *Plasma Phys. Control. Fusion* **26** 209

[12] Hively L M 1977 *Nucl. Fusion* **17** 873

[13] Lazarus E A *et al* 1997 *Nucl. Fusion* **37** 7

[14] Gates D A and the NSTX National Research Team 2003 *Phys. Plasmas* **15** 1659

[15] Janeschitz G *et al* 2000 *Nucl. Fusion* **40** 1197

[16] Kessel C E 1994 *Nucl. Fusion* **34** 1221

[17] Hirshman S P 1988 *Phys. Fluids* **31** 3150

[18] Gong X Y, Shi B R and Long Y X 2003 *Acta Phys. Sin.* **52** 896 (in Chinese)

[19] Gong X Y, Shi B R, Zhang J H *et al* 2002 *Acta Phys. Sin.* **51** 2547 (in Chinese)